Inhibition of Carbon Steel Corrosion by Some New Organic 2-Hydroselenoacetamide Derivatives in HCl Medium

Alaa Abdel Khaleq Khalib[1], Hanan Abdul Jaleel Al-Hazam[2], and Attared Fadhel Hassan[2*]

[1]*Iraqi Cement State Company, Basrah, Iraq*

[2]*Department of Chemistry, College of Science, University of Basrah, Basrah 61004, Iraq*

Abstract: *This study aims to prepare 2-hydroselenoacetamide derivatives (5-8) to use some of these compounds as corrosion inhibition for carbon steel in 1 M HCl. The compound $C_{10}H_{10}NO_2Cl$ 1 was prepared by reacting between p-aminoacetophenone with chloroacetyl chloride, and then reacted 1 with substituted benzaldehyde to obtain the corresponding derivatives as $C_{17}H_{13}N_2O_4Cl$ 2, $C_{18}H_{16}NO_4Cl$ 3 and $C_{19}H_{18}NO_4Cl$ 4. The last step in this study was conducted to obtain the organic hydroselenoacetamide such as $C_{10}H_{11}NO_2Se$ 5, $C_{17}H_{14}N_2O_4Se$ 6, $C_{18}H_{17}NO_4Se$ 7, and $C_{19}H_{19}NO_4Se$ 8 by reacting chloroaminochalcone and sodium hydrogen selenide. All compounds were characterized by Fourier Transform Infrared Spectroscopy (FTIR), proton nuclear magnetic resonance (^{1}H-NMR), and elemental analysis (CHN). The corrosion inhibition activity of $C_{17}H_{14}N_2O_4Se$ 6, $C_{18}H_{17}NO_4Se$ 7 and $C_{19}H_{18}NO_4Cl$ 4 for carbon steel in 1 M HCl solution was investigated by using weight loss methods and electrochemical study. The activation energy of the corrosion reaction was also calculated. The effect of different concentrations and temperatures on inhibition efficiency was investigated. The results showed that the corrosion rate decreased with the increase of the concentration of inhibitors, while the inhibition efficiency and covered area decreased with an increase in the temperature. Polarization studies demonstrated that the inhibitors were of mixed type. The purpose of this study was to prepare, characterize and evaluate the corrosion inhibition activity of hydroselenide compounds for carbon steel in 1 M HCl.*

Keywords: *corrosion inhibition; 2-hydroselenoacetamide; chalcone; acid medium*

■ INTRODUCTION

The composition of the amides has attracted considerable attention from researchers because of their importance in biochemistry and organic chemistry fields, their usage as intermediate compounds in organic synthesis, and wide range of industrial chemical applications [1]. The association of amide is significant as it plays as the main component of peptides, polymers, natural compounds products, and pharmaceuticals [2]. Many amide derivatives have been used as antifungals, antihistamines, worms, and antibacterial agents. For example, the compound *N*-aryl-2-chloroacetamides acts as an antimicrobial such as herbicides, antifungals, and disinfectants [3].

The chloroacetylation of *p*-aminoacetophenone with chloroacetyl chloride occurred in the presence of glacial acetic acid [4] or in benzene and trimethylamine [5] to give the compound no. **1** as shown in Scheme 1. The *N*-substituted chloroacetamides could be converted to chalcones through Claisen-Schmidt condensation [6]. Mostly chalcones are aromatic ketones that consist of two aromatic rings that are linked by a three-carbon α,β unsaturated carbonyl system. Chalcone has a complete delocalization π- electron system on conjugated double bond (C=C) and two phenyl rings. Therefore, the redox potential for the molecules decreases while their stability increases [7]. The Claisen-Schmidt condensation is a crossed aldol condensation reaction between ketone
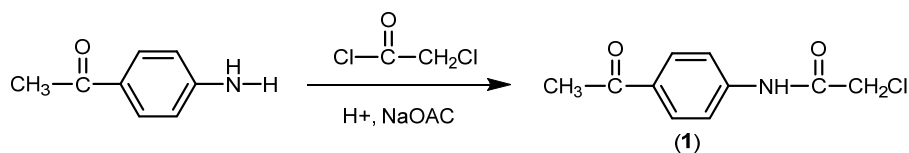
Scheme 1. Synthesis of *N*-aryl chloroacetamide (**1**)

possessing at least one α-hydrogen with the aldehyde. The reaction is proceeded via the base-catalyzed formation of enolate of the ketone. This enolate attacks the aldehyde carbon and forms the adduct. Chalcone is then formed from this adduct by the elimination of water molecule [8].

Selenium and its organic compounds are of great interest due to their various applications in some industrial fields, for example, platinum group metal complexes of seleno ligand were developed as catalysts for different reactions [9-10]. Metal selenolates exhibit as versatile single–sources of molecular precursors for the synthesis of nanoparticles and deposition of thin films of metal selenides [11-13]. Selenium and its compounds are used as oxidizing agents for organic compounds [14]. Selenium can be introduced as a nucleophile/electrophile or even as a radical in chemo–, regio– and stereo–selective manners [15].

Selenol is an organic compound that contains C-Se-H functional group, sometimes called selenothiols or selenomercaptans. Selenols are more acidic than corresponding sulfur analogous because the energy of Se-H bond is weaker than S-H bond and thus oxidized easily and serve as Hydrogen atom donors. The RSe^- is a good nucleophile as well as an excellent leaving group. Also, it binds metal strongly, which is used for heavy metal detoxification [16]. There are different methods for the synthesis of selenols or selenolates [17-18], one of these methods is the reaction of organic halides with sodium hydrogen selenides or sodium selenides [19], as shown in Scheme 2.

Corrosion is a process of gradual damage to material (mostly metals) through a chemical reaction with their environment, causing the outer surface of the metal to change and breaking down the crystal structure and dissolution in the outer environment. It is a continuous process that cannot be stopped, but it can be reduced by using various preventive systems, including the use of organic compounds, which can easily be adsorbed onto the steel surface and lead to the formation of a protective organic film on the electrode surface and reduce the corrosion rate [20]. The efficiency of organic compounds as an inhibitor mainly depends on the presence of elements of groups V and VI of the periodic table, such as N, P, As, S, O, and Se, which have lone electron pairs, and the conjugated system as well as the presence of π-electrons in their structure which can strongly be adsorbed on the metal surface through to donor-acceptor process to form a protective layer [21-22]. Some organic compounds have been synthesized and evaluated as corrosion inhibition in acidic media containing heteroatoms, and the conjugated system enhances the chemical adsorption process involving electrons sharing between the vacant d-orbitals of iron and the lone electron pairs of the heteroatoms to create a strong coordinating bond which improves anti-corrosion performance [21-23]. The aim of this study is to prepare and characterize some novel organic seleno compounds and use them as corrosion inhibition for carbon steel in a 1 M HCl solution.

■ **EXPERIMENTAL SECTION**

Materials

The chemicals included *p*-amino acetophenone, 4-nitrobenzaldehyde, 3,5-dimethoxybenzaldehyde, and

X= substituents
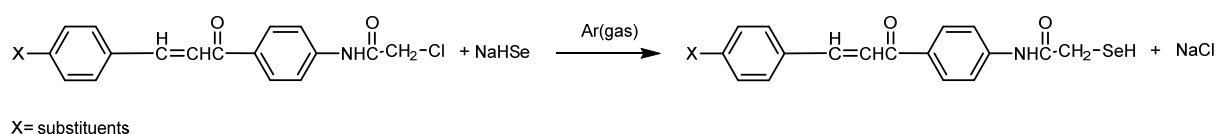
Scheme 2. Synthesis 2-hydroseleno-*N*-arylacetamide

sodium acetate were purchased from Merck. Meanwhile, glacial acetic acid, ethanol, toluene, trimethylamine (Sinopharm Chemical Reagent Co., Ltd.), chloroacetyl chloride, sodium borohydride (Sigma Aldrich), selenium powder, 3-hydroxybenzaldehyde (Alpha) were also utilized in this study. All chemicals were used as received with no purification. Carbon steel specimens were used in this work had the composition of (wt.%) [Fe:99.68, C:0.037, Mn:0.26, P:0.005, S:0.002]. The specimens were rubbed successively using emery with grade 600 to 1200 mesh/min, then washed with distilled water, cleaned with acetone then fired in a hot air blower. The working electrode was a 7.5 cm long steam for electrochemical measurement to provide an exposed surface area of 1.0 cm^2, while 2.5 × 2.0 × 0.2 cm^3 were used in weight loss measurements. The 1 M HCl test solution was prepared from analytical grade reagent (37%) and deionized water.

Instrumentation

The elemental analysis of new synthesis compounds was done by (CE-440) Elemental Analyzer. The IR spectra were measured using FTIR-8400S SHIMADZU-Japan and ^{1}H-NMR was recorded on BUKER (300 MHz) with DMSO-d$_6$ solvent. All melting points were measured with a Gallen Kamp melting point apparatus and uncorrected. The progress of the reaction was monitored with thin-layer chromatography (TLC).

Procedure

Synthesis N-(4-acetylphenyl)-2-chloroacetamide (1)
Prepared *N*-acetylphenyl-2-chloroacetamide (1) by two methods. A solution of chloroacetyl chloride (1.13 mL) in glacial acetic acid was added to 1.35 g *p*-aminoacetophenone in 10 mL glacial acetic acid at room temperature, the solution was stirred for 30 min, and then CH$_3$COONa (10 mL) 0.5 M was added to the mixture with constant stirring for another 30 min. The crude product was filtered, dried, and then recrystallized by ethanol [4].

A mixture of *p*-aminoacetophenone (1.35 g) with chloroacetyl chloride (1.19 mL) in 25 mL of toluene was added 3–4 drops of triethylamine. The mixture solution was refluxed for 4 h. The progress of the reaction was monitored by TLC with the mobile phase of toluene: acetone (7:3). A buff-colored solid-state intermediate was

obtained and recrystallized by toluene [24].

Synthesis 2-chloro-N-(4-(3-(4-X-phenyl)acryloyl)phenyl)acetamide (2)

The mixture of equimolar quantities of (**1**) (2.11 g) *N*-(4-acetylphenyl)-2-chloroacetamide with substituted benzaldehyde (**2**), i.e., 4-nitrobenzaldehyde (1.51 g), (**3**) 3,4-dimethoxybenzaldehyde (1.67 g), (**4**) 3-hydroxy benzaldehyde (1.22 g) in ethanol was added by 20% sodium hydroxide solution slowly dropwise with stirring. After completing the addition, stirring continued for 6 h and then left overnight. The mixture was added to ice water, and then measured the pH of the solution. The obtained product was recrystallized from ethanol [25].

Synthesis 2-hydroseleno-N-(4-(3-(4-X-phenyl)acryloyl) phenyl)acetamide

The NaBH$_4$ (0.225 g: 0.0061 mol) was dissolved in 25 mL H$_2$O then added Se 0.23 g: 0.0029 mol while stirring and suspended in 25 mL H$_2$O under argon atmosphere. A severe reaction occurred in less than 10 min, and H$_2$ gas was immediately released. A colorless solution of sodium hydrogen selenide NaHSe was formed.

Solution of NaHSe was added to 2-chloro-*N*-(4-(3-(4-X-phenyl)acryloyl)phenyl)acetamide 2.09 g: 0.0061 mol in 50 mL absolute ethanol, after about 45 min stirred,
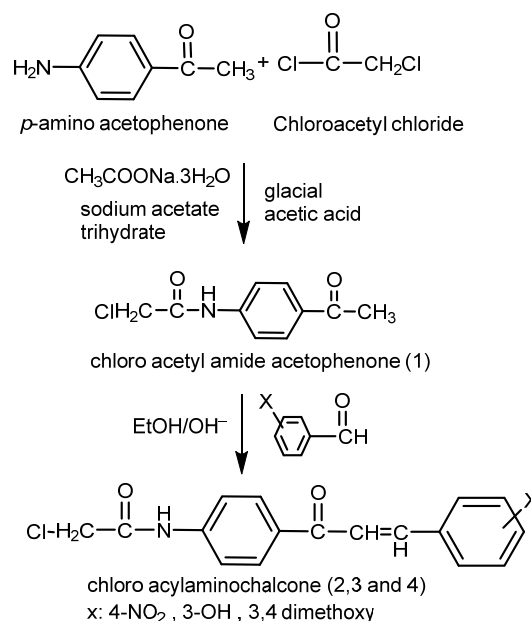
Scheme 3. Preparation of chloroaminochalcone
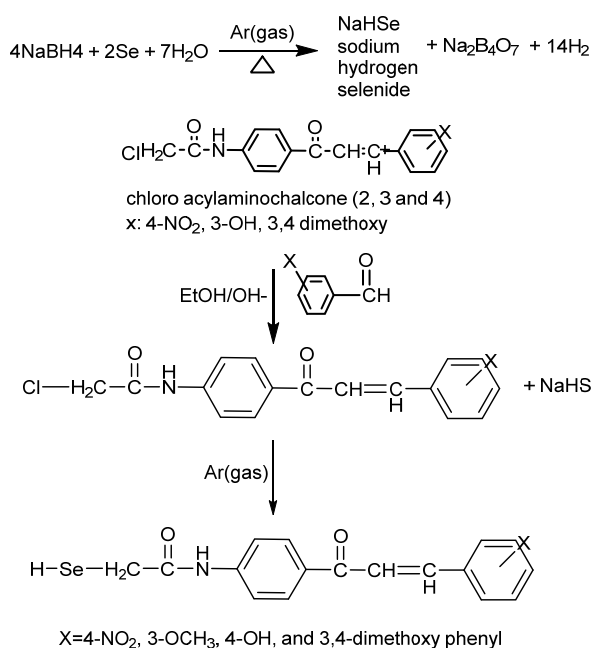
Scheme 4. Preparation of 2-hydroseleno-*N*-(X-phenyl)acryloyl)phenyl)acetamide

the reddish color precipitate was obtained, filtered, and washed several times with ethanol and dried (Schemes 3 and 4).

N-(4-Acetylphenyl)-2-chloroacetamide as compound 1. Off-white. Yield: 90%. m.p 153–155 °C. IR ν cm^{-1} (KBr): 3286 (NH 2°-amide), 1654 (C=O amide), 725 (C-Cl). ^{1}H-NMR spectra (ppm) DMSO-d_6 solvent: 10.65 (1H, NH amide), 7.72 (4H aromatics), 4.34 (2H CH$_2$), 2.55 (3H CH$_3$). Anal. calc. for C$_{10}$H$_{10}$NO$_2$Cl: C, 56.75; H, 4.76; N, 6.62. Found: C, 56.16; H, 4.49; N, 6.36.

2-Chloro-I-(4-(3-(4-nitrophenyl)acryloyl)phenyl)-2-chloroacetamide as compound 2. Brown. Yield: 70%. m.p 200–202 °C. IR ν cm^{-1} (KBr): 3387 (NH amide), 1697 (C=O amide), 1635 (C=O chalcone), 632 (C-Cl). ^{1}H-NMR spectra (ppm) DMSO-d_6 solvent: 6.72 (1H NH amide), 7.69 (8H aromatics), 3.39 (2H CH$_2$), 6.54 (2H CH=CH). Anal. calc. for C$_{17}$H$_{13}$N$_2$O$_4$Cl: C, 59.23; H, 3.80; N, 8.13. Found: C, 58.96; H, 3.72; N, 7.96.

2-Chloro-*N*-(4-(3-(4-hydroxy-3-methoxyphenyl) acryloyl)phenyl)acetamide as compound 3. Brown. Yield: 40%. m.p 185–188 °C. IR ν cm^{-1} (KBr): 3394 (1H NH amide), 1681 (C=O amide), 1651 (C=O chalcone), 702 (C-Cl). ^{1}H-NMR spectra (ppm) DMSO-d_6 solvent: 9.78 (NH amide), 6.95 (8H aromatics), 2.64 (2H CH$_2$),

3.95 (3H OCH$_3$). Anal. calc. for C$_{18}$H$_{16}$NO$_4$Cl: C, 62.52; H, 4.66; N, 4.05; Found: C, 61.99; H, 4.65; N, 3.9.

2-Chloro-*N*-(4-(3-(3,4-dimethoxyphenyl)acryloyl) phenyl)acetamide as compound 4. Yellow. yield: 80%. m.p 138–140 °C. IR ν cm^{-1} (KBr): 3352 (NH amide), 1643 (C=O amide), 1600 (C=O chalcone), 721 (C-Cl). ^{1}H-NMR spectra (ppm) DMSO-d_6 solvent: 7.97 (1H NH amide), 6.13 (8H aromatics), 3.36 (2H CH$_2$), 3.83 (6H 2(OCH$_3$)). Anal. calc. for C$_{19}$H$_{18}$NO$_4$Cl: C, 3.42; H, 5.04; N,.89; Found: C, 62.96; H, 5.11; N, 3.6.

N-(4-Acetylphenyl)-2-hydroselenoacetamide as compound 5. Off-white. Yield: 70%. m.p 190–192 °C. IR ν cm^{-1} (KBr): 3348 (NH amide), 1651 (C=O amide), 2370 (Se-H). ^{1}H-NMR spectra (ppm) DMSO-d_6 solvent: 10.97 (1H NH 2° amide), 7.75 (4H aromatic), 3.36 (2H CH$_2$ + 1H Se-H), 2.48 (3H CH$_3$). Anal. calc. for C$_{10}$H$_{11}$NO$_2$Se: C, 46.89; H, 4.33; N, 5.47. Found: C, 46.49; H, 3.92; N, 5.16.

2-Hydroseleno-*N*-(4-(3-(4-nitrophenyl)acryloyl) phenyl)acetamide as compound 6. Dark red. Yield: 60%. m.p 213–215 °C. IR ν cm^{-1} (KBr): 3383 (NH amide), 1635 (C=O amide), 1600 (C=O chalcone), 2470 (Se-H). ^{1}H-NMR spectra (ppm) DMSO-d_6 solvent: 9.88 (1H NH amide), 7.14 (8H aromatics), 4.38 (2H CH$_2$ + 1H Se-H), 6.54 (2H CH=CH). Anal. calc. for C$_{17}$H$_{14}$N$_2$O$_4$Se: C, 52.45; H, 3.63; N, 7.20. Found: C, 52.13; H, 4.14; N, 7.03.

2-Hydroseleno-*N*-(4-(3-(4-hydroxy-3-methoxyphenyl)acryloyl)phenyl)acetamide as compound 7. Dark red. Yield: 41%. IR ν cm^{-1} (KBr): 3406 (NH amide), 1735 (C=O amide), 1654 (C=O chalcone), 2340 (Se-H). ^{1}H-NMR spectra (ppm) DMSO-d_6 solvent: 8.66 (1H NH amide), 6.53 (8H aromatics), 4.30 (2H CH$_2$ + 1H Se-H), 3.76 (3H OCH$_3$). Anal. calc. for C$_{18}$H$_{17}$NO$_4$ClSe: C, 55.39; H, 4.39; N, 3.59. Found: C, 54.93; H, 4.55; N, 3.40.

2-Hydroseleno-*N*-(4-(3-(3,4-dimethoxyphenyl) acryloyl)phenyl)acetamide as compound 8. Dark red. Yield: 60%. IR ν cm^{-1} (KBr): 3363 (NH amide), 1658 (C=O amide), 1610 (C=O chalcone), 2340 (Se-H). ^{1}H-NMR spectra (ppm) DMSO-d_6 solvent: 8.72 (1H NH amide), 7.42 (8H aromatics), 3.36 (2H CH$_2$ + 1H Se-H), 2.52 (6H 2(OCH$_3$)). Anal. calc. for C$_{19}$H$_{19}$NO$_4$Se: C, 56.44; H, 4.74; N, 3.46. Found: C, 55.99; H, 4.69; N, 3.11.

Corrosion activity

Weight loss method. The weight loss measurements have been used to investigate the corrosion behavior of carbon steel alloy in the presence and absence of inhibitors. The inhibition efficiency (η%) and surface coverage (θ) were calculated by the Eq. (1) and (2)

$$\eta\% = \frac{C_R - C_{Ri}}{C_R} \times 100 \tag{1}$$

$$\theta = \frac{C_R - C_{Ri}}{C_R} \tag{2}$$

where C_R = Corrosion rate in absence of organic hydroselenide compounds, C_{Ri} = corrosion rate values in presence of hydroselenide compounds. The C_R of carbon steel was calculated in acidic medium by the Eq. (3)

$$C_R = \frac{\Delta W}{At} \tag{3}$$

where ΔW = weight loss for the ingot (mg), A = the area of the submerged surface of the specimen (cm²), t = the time of immersion (h).

Electrochemical measurements (Tafel method). The potentiodynamic polarization (PDP) with computer-controlled potentiostat (model Corr Test-(5350) was used to perform electrochemical measurements. It examines the corrosion of carbon steel alloy in 0.1 M HCl solution in the absence and presence of a different concentration of inhibitor 2-chloro-*N*-(4-(3-(3,4,-dimethoxyphenyl) acryloyl)phenyl)acetamide and 2-hydroseleno-*N*-(4-(3-(4-nitrophenyl)acryloyl)phenyl)acetamide compounds at room temperature and different concentration of inhibitors, or at different temperatures and a concentration 100 ppm of inhibitors.

Electrochemical cell. In this study, an electrochemical cell consisting of three electrodes arranged as follows: The working electrode which represents alloy carbon steel with dimensions of (5 × 1.5 × 0.2) cm³, which represents the submerged part of the alloy. Platinum Auxiliary Electrode and Saturated Calomel Electrode (SCE) with a fiber–loggin capillary represent as a Reference Electrode (RE). The device is programmed by entering information that includes the data of measurement, the thickness of the ingot, the type of operation, the equivalent weight of the metal, the type and density of the metal. The time required to conduct an examination is about 20 min, after which the cell and loggin tube is emptied, and the process is repeated three times to ensure the accuracy of the results. The examination process is carried out in the absence and presence of different concentrations of inhibitors. The corrosion rate C_{Rmpy} was evaluated from Eq. (4).

$$C_{Rmpy} = \frac{0.13 \times I_{corr} \times Eq.wt}{A \times D} \tag{4}$$

where I_{corr} is corrosion current density in μA cm⁻², Eq.wt is the equivalent weight of the specimen, A is the total specimen area, and D is the density of the specimen.

■ RESULTS AND DISCUSSION

CHN Measurement

All the prepared compounds showed agreement with the practical and theoretical results of elemental (CHN) analysis, indicating the validity of the proposed chemical structures for the prepared compounds. All results of CHN analysis are listed in Table 1.

Table 1. The CHN data of selected compounds

No.	Empirical formula	Elemental analysis found (calc)		
		% C	% H	% N
1	$C_{10}H_{10}NO_2Cl$	56.16(56.75)	4.49(4.76)	6.36(6.62)
2	$C_{17}H_{13}N_2O_4Cl$	58.96(59.23)	3.72(3.80)	7.96(8.13)
3	$C_{18}H_{16}NO_4Cl$	61.99(62.52)	4.65(4.66)	3.90(4.05)
4	$C_{19}H_{18}NO_4Cl$	62.96(63.42)	5.11(5.04)	3.69(3.89)
5	$C_{10}H_{11}NO_2Se$	46.49(46.89)	3.92(4.33)	5.16(5.47)
6	$C_{17}H_{14}N_2O_4Se$	52.13(52.45)	4.14(3.63)	7.03(7.20)
7	$C_{18}H_{17}NO_4Se$	54.93(55.39)	4.55(4.39)	3.40(3.59)
8	$C_{19}H_{19}NO_4Se$	55.99(56.44)	4.69(4.74)	3.11(3.46)

FTIR Spectra

The FTIR spectra for chalcones and their hydroselenides have been studied and analyzed in terms of functional groups. The FTIR spectrum of compounds **1**-**4** exhibited strong absorption bands that appeared at 3286–3394 and 1643–1697 cm^{-1} belonging to stretching vibration for N-H and C=O, respectively [26]. The absorption bands appear at 632–725 cm^{-1} and belong to C-Cl stretching vibration for 2-chloro-*N*-phenylacetamide derivatives [27]. The absorption bands around 1600–1651 cm^{-1} related to the carbonyl group conjugated with double bond, which indicates the formation of chalcones [28-29].

The FTIR spectrum for compounds **5**-**8** shows absorption band appears at 532–640 and 2340–2470 cm^{-1} belonging to stretching vibration for C-Se and Se-H indicating to formation 2-hydroselenide [30-31], other unsymmetrical stretching vibration for C=C aromatic, C-H aliphatic, C-H aromatic, and C=C aliphatic were found at expected positions [28-29]. Fig. 1 showed the IR-spectra of compound **6**.
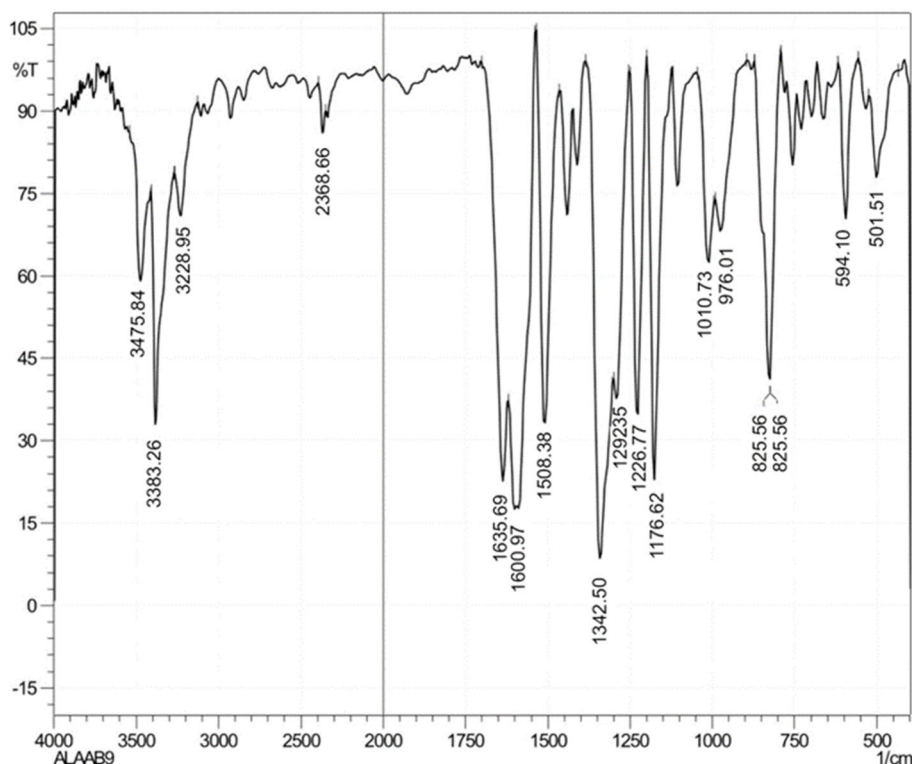
^{1}H-NMR Spectra

^{1}H-NMR spectra of compounds **1**-**4** displayed signals at 7.97–10.68 ppm belonging to NH amide [32], phenyl protons and alkene protons give multiple signals extent 6.13–8.35 ppm [30], also methylene protons appear at 3.36–4.33 ppm [34] in the low field because methylene groups attached chloride atom; high electronegativity, that increase chemical shift.

The compounds **5**-**8** displayed signals at 8.66–10.97 ppm belonging to NH amide. Methylene protons and the proton of Se-H group appears at 3.36–4.45 ppm [35] at the high field because of the disappearance chloride atom and are attached to the selenium atom, which is less electronegativity than the chloride atom. Fig. 2. The ^{1}H-NMR for compound **5**.

Weight Loss Studies

Effect of inhibitor concentration

In this study, the weight loss method was used to evaluate the effect of corrosion of carbon steel immersed in 1 M hydrochloric acid solution for 48 h at 300 K.
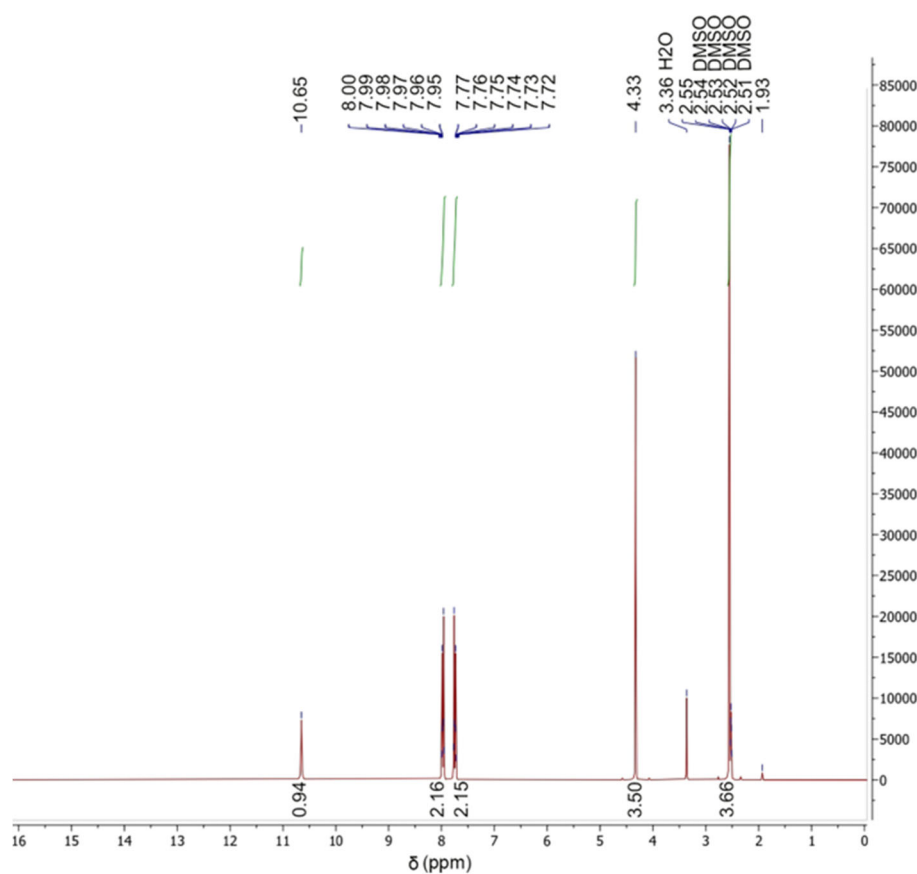

Fig 1. The FTIR spectra of compound **6**

Fig 2. The ^{1}H-NMR for compound **5**

Table 2. Weight loss method results for carbon steel alloy in different concentrations at 300 K

Inhibitors	Inhibitors concentration (ppm)	C_R (mg cm^{-2} h^{-1})	θ	$\eta\%$
(0) inhibitor	0.0	0.0138	-	-
$C_{18}H_{17}NO_4Se$ (**7**)	50	0.0113	0.3864	38.64
	100	0.0106	0.4270	42.70
	150	0.0096	0.4783	47.83
	200	0.0092	0.4994	49.94
	300	0.0091	0.5081	50.81
$C_{17}H_{14}N_2O_4Se$ (**6**)	50	0.0136	0.2648	26.48
	100	0.0126	0.3189	31.89
	150	0.0111	0.4000	40.00
	200	0.0103	0.4432	44.32
	300	0.0095	0.4864	48.64

Different concentrations of selenides lead to different values of $\eta\%$, C_R, and θ were listed in Table 2. The increase of hydroselenide concentration causes the increase of $\eta\%$ at 300 K.

The obtained result showed that the hydroselenide compounds **6** and **7**, which are used as inhibitors in this study, inhibit the corrosion of carbon steel in the acidic medium. It is noted that the corrosion rate decreased, and the inhibitor efficiency increased with the increasing concentration of inhibitors, as shown in Table 2. These

results show that the presence of an inhibitor works to form a thin layer that protects the anodic and cathodic region and works to reduces oxidation reaction, and limits corrosion processes by preventing the arrival of corrosion to the surface of carbon steel [20-23].

The action of inhibitors can be explained by the molecular adsorption of inhibitors on the surface of the alloy. The effective adsorption is a result of the interact of π-electrons of multiple bonds and aromatic system of inhibitor molecules with the metal, or interaction of lone pair electron present on highly electronegative atoms (N and O) in the structure of inhibitors molecules with d-orbital of iron [21-23,33].

Referring to Table 2, we find that the inhibition efficiency of compound **7** (50.81%) is higher than that of compound **6** (48.64%) at the same concentration, 300 ppm, as shown in Fig. 3, due to the presence of electron releasing groups, –OH and –OCH$_3$, compared to the electron-withdrawing (–NO$_2$) group in compound **6**. So that the electron density on the phenyl ring in compound **7** is higher, which improves the adsorption process and increases the surface area covered by the inhibitor, unlike compound **6**, where the presence of the electron-withdrawing group reduces the electron density on the phenyl group, reducing the adsorption process and thus reducing the efficiency of the inhibitor [21-23].

Effect of temperature on inhibition efficiency

A weight-loss experiment has been performed in the temperature range between 300–320 K in the presence and absence of optimum concentration of inhibitors. Table 3 lists corrosion rate (C$_R$), inhibition efficiency (η%) and surface coverage (θ) at each temperature.
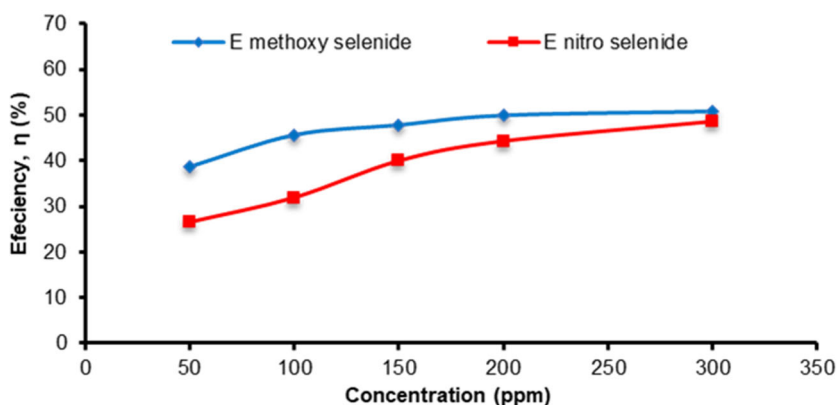

Fig 3. Relationship between inhibitor efficiency with increasing inhibitor concentration for nitro selenide (**6**) and methoxy selenide (**7**)

Table 3. Weight loss results for carbon steel alloy in different grades and at a concentration of 100 ppm of inhibitors in 1 M HCl

Inhibitors	Temperature (K)	C$_R$ (mg cm^{-2} h^{-1})	θ	η%
(0) inhibitor	300	0.0138	-	-
	310	0.0143	-	-
	320	0.0225	-	-
	300	0.0049	0.6415	64.15
C$_{18}$H$_{17}$NO$_4$Se (**7**)	310	0.0068	0.5261	52.61
	320	0.0113	0.4977	49.77
	300	0.0066	0.5171	51.71
C$_{17}$H$_{14}$N$_2$O$_4$Se (**6**)	310	0.0083	0.4216	42.16
	320	0.0156	0.3066	30.66

In general, it can be seen that the increase in the temperature leads to an increase in the corrosion rate from 0.01367 mg cm^{-1} h^{-1} at 300 K to 0.0225 mg cm^{-1} h^{-1} at 320 K in the absence of inhibitor, and from (0.0066, 0.0048) mg cm^{-1} h^{-1} at 300K to (0.0113, 0.0156) mg cm^{-1} h^{-1} at 320 K for inhibitor **6** and **7**, respectively. Also, inhibition efficiency decreased with an increase in the temperature of the corrosion medium when the concentration was fixed, as shown in Fig. 4. This behavior is because the increase in temperature in the absence of an inhibitor increases the kinetics of the anodic and cathodic reactions, and the dissolution of metal becomes more important, as shown in Table 3 [22]. In the case of the presence of the inhibitor, the corrosion rate will increase but less than in the absence of inhibitor. This is because

the high temperature leads to an increase in the kinetic energy of inhibitor molecules and an increase in their diffusion, which reduces the efficiency of adsorption of the inhibitor on the surface of carbon steel as well as reduces the surface area covered by the inhibitor molecules which may be formed by heterogeneous layer [22,34-35].

Polarization Studies (Tafel Method)

The inhibition process of inhibitors **4** and **6** for corrosion of carbon steel in HCl 1 M at 300 K was studied by polarization experiments. The electrochemical parameter values are listed in Table 4. Fig. 5 shows the relationship between the corrosion efficiency and the concentration of inhibitors.
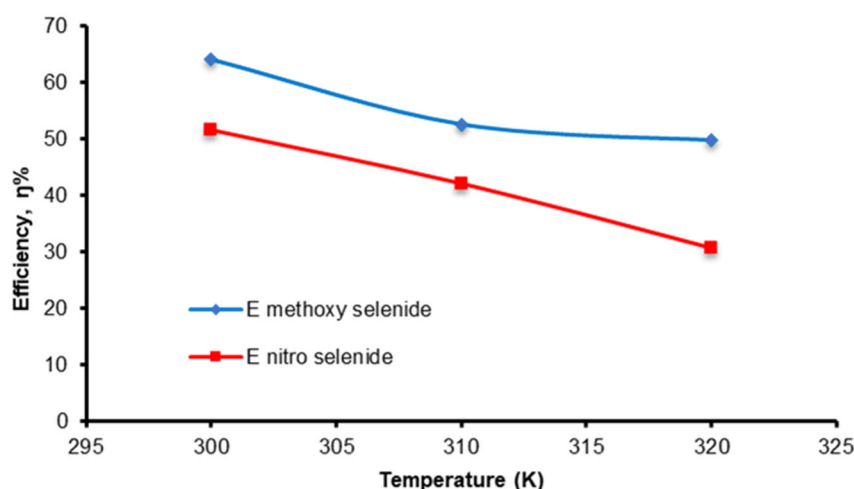

Fig 4. Relationship between the inhibition efficiency and temperature of the corrosion medium

Table 4. Tafel method results for carbon steel alloy in different concentrations of inhibitors in 1 M HCl at 300 K

| Inhibitors	Inhibitors concentration (ppm)	E_{corr} (mV)	I_{corr} (μ A cm^{-2})	C_R M$_{py}$	(%η)
(0) inhibitor	0.1 M	-0.54373	91.99	2.46	-
C$_{19}$H$_{18}$NO$_4$Cl (**4**)	50	-0.53325	81.44	2.18	11.38
	100	-0.50546	69.37	1.85	24.79
	150	-0.51232	77.44	2.07	15.85
	200	-0.50032	67.09	1.79	27.23
	300	-0.50677	57.15	1.52	38.21
C$_{17}$H$_{14}$N$_2$O$_4$Se (**6**)	50	-0.54465	67.55	1.80	26.82
	100	-0.50742	63.33	1.69	31.30
	150	-0.50086	55.86	1.49	39.26
	200	-0.51166	58.73	1.57	36.17
	300	-0.51200	49.37	1.32	46.34
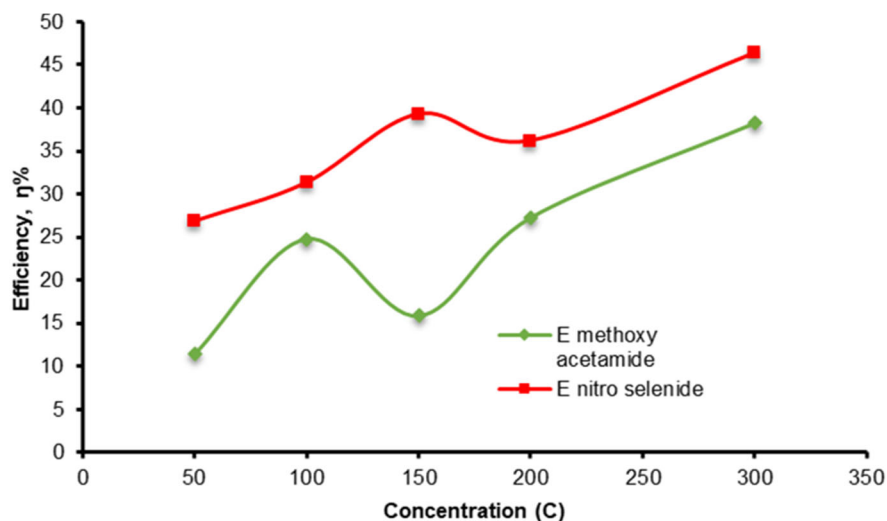
Fig 5. Relationship between the inhibition efficiency and concentration of the corrosion medium
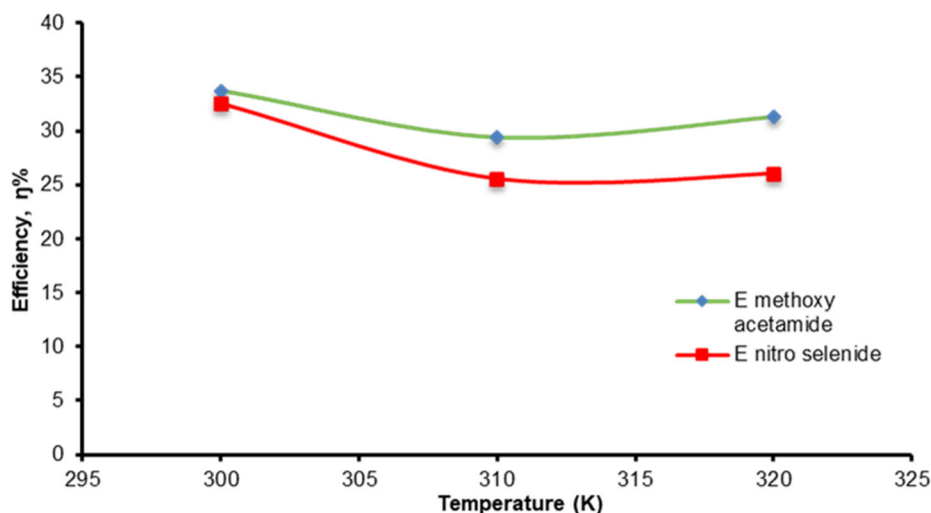

Fig 6. Relationship between the inhibition efficiency and temperature of the corrosion medium at 100 ppm

Referring to Table 4, it is evident that the value of corrosion current density is high in the absence of the inhibitor and decreases significantly with the addition of inhibitors; thus, the corrosion rate decreases. From the values of E_{corr}, it is noted that the behavior of both inhibitors is of a mixed type [36]. It shows in Fig. 5, which represents the Tafel curve for compounds **4** and **6**. The optimum concentration of both inhibitors **4** and **6** are 300 ppm, where the inhibition efficiency reached 38.21 and 46.34%, respectively.

Through the results obtained in Table 4 and Fig. 5, we note that the use of organoselenium inhibitor **6** gives a higher inhibition efficiency, 46.34%, than the chalcone (**4**)

(38.21%) at 300 ppm. The reason is due to the presence of Se heteroatoms in compound **6** which enhances the adsorption process on the surface of the alloy through the sharing between the lone electron pairs of the Se atom and empty d-orbital of iron to establish a strong coordinated bond [37].

Effect of temperature on inhibition efficiency

The effect of temperature on inhibition efficiency was studied at 300–320 K in the absence and presence of inhibitors by the Tafel method. The results are listed in Table 5. Fig. 6 shows the relationship between the inhibition efficiency and the temperature of the corrosion medium. Table 4 shows an increase in the I_{corr}

Table 5. Tafel method results for carbon steel alloy in 1 M HCl at different temperatures and 100 ppm of inhibitors

Inhibitors	Temperature (K)	E_{corr} (mV)	I_{corr} (μ A cm^{-2})	C_R M_{py}	(%η)
(0) inhibitor	300	-0.54373	191.99	2.46	-
	310	-0.54440	250.11	6.69	-
	320	-0.53933	290.11	7.76	-
$C_{19}H_{18}NO_4Cl$ (**4**)	300	-0.50677	127.15	3.40	33.72
	310	-0.50131	156.448	4.72	29.44
	320	-0.49248	199.16	5.33	31.31
$C_{17}H_{14}N_2O_4Se$ (**6**)	300	-0.51200	149.37	3.46	32.55
	310	-0.50121	182.14	4.87	27.20
	320	-0.50093	214.66	5.74	26.03

and, consequently, an increase in the corrosion rate with an increase in temperature from 300–320 K, which led to a decrease in the inhibition efficiency due to the dissolution of inhibitor layer adsorbed on the surface of the alloy as shown in Fig. 6.

The activation energy E_a of corrosion reaction in the absence and presence of inhibitors was calculated by the Arrhenius equation (5).

$$\ln C_R = \ln A - \frac{E_a}{RT} \qquad (5)$$

C_R is corrosion rate, A is the Arrhenius constant, T is absolute temperature, and R is the gas constant. Values of activation energy can be determined from the slope of the plots of ln C_R vs. 1/T. The values of E_a are 17.68, 20.419 and 23.75 kJ/mol in the absence, presence of inhibitors **4** and **6**, respectively. These values are less than 80 kJ/mol required for chemical adsorption. It can be concluded from the calculated E_a values that the adsorption of inhibitors is a physical type [38].

■ CONCLUSION

The corrosion inhibition performance of new organic hydroselenide derivatives of carbon steel in HCl 1 M solution was evaluated using weight loss technique and electrochemical studies. The result obtained showed that the inhibitors are classified as mixed-type. The corrosion rate decreases and the inhibition efficiency increases with the increase in the concentration of inhibitors. The inhibition efficiency and covered area decrease with increasing corrosion medium temperature in the absence and presence of an inhibitor. The study also showed that the inhibition efficiency of compound **7** is higher than

that of compound **6** due to the presence of –OH and –OCH$_3$ electron releasing groups on the benzene ring, which enhances the ability of adsorption of inhibitor on the surface of the alloy. From the calculated activation energy values of 17.68, 20.419, and 23.75 kJ/mol in the absence and presence of inhibitors, the adsorption process was classified as physical adsorption.

■ REFERENCES

[1] Olivares-Xometl, O., Likhanova, N.V., Domınguez-Aguilar, M.A., Hallen, J.M., Zamudio, L.S., and Arce, E., 2006, Surface analysis of inhibitor films formed by imidazolines and amides on mild steel in an acidic environment, *Appl. Surf. Sci.*, 252 (6), 2139–2152.

[2] Abdel-Latif, E., Fahad, M.M., El-Demerdash, A., and Ismail, M.A., 2020, Synthesis and biological evaluation of some heterocyclic scaffolds based on the multifunctional *N*-(4-acetylphenyl)-2-chloroacetamide, *J. Heterocycl. Chem.*, 57 (8), 3071–3081.

[3] Abdel-Latif, E., Fahad, M.M., and Ismail, M.A., 2020, Synthesis of *N*-aryl 2-chloroacetamides and their chemical reactivity towards various types of nucleophiles, *Synth. Commun.*, 50 (3), 289–314.

[4] Jayaramu, P.K., and Maralihalli, R.R., 2015, Synthesis and *in vitro* biological activities of chalcones and their heterocyclic derivatives, *Pharma Chem.*, 7 (8), 30–35.

[5] Shukla, M.B., Mahyavanshi, J.B., and Parmar, K.A., 2016, Synthesis and antimicrobial activities of

various *N*-phenyl-2-{[5-(3,4,5-trimethoxyphenyl)-1,3,4-oxidiazol-2-yl]sulfanyl}acetamides, *Indian J. Chem.*, 55B, 374–380.

[6] Velikorodov, A.V., Ionova, V.A., Temirbulatova, S.I., Titova, O.L., and Stepkina, N.N., 2013, Synthesis and application of chalcones to the preparation of heterocyclic structures, *Russ. J. Org. Chem.*, 49 (11), 1610–1616.

[7] Gaonkar, SL., and Vignesh, U.N., 2017, Synthesis and pharmacological properties of chalcones: A review, *Res. Chem. Intermed.*, 43 (11), 6043-6077.

[8] Gupta, J.K., Singh, S.V., and Gupta, K.R., 2017, Chalcones: A review on synthesis, chemical properties and biological activities, *Res. Pharm.*, 1 (2), 1–10.

[9] Yao, Q., Kinney, E.P., and Zheng, C., 2004, Selenium–ligated palladium(II) complexes as highly active catalysts for carbon-carbon coupling reactions: The Heck reaction, *Org. Lett.*, 6 (17), 2997–2999.

[10] Kumar, A., Rao, G.K., Saleem, F., and Singh A.K., 2012, Organoselenium ligands in catalysis, *Dalton Trans.*, 41 (39), 11949–11977.

[11] Bochmann, M., 1996, Metal chalcogenide materials: Chalcogenolato complexes as "single-source" precursors, *Chem. Vap. Deposition*, 2 (3), 85–96.

[12] Jain, V.K., 2019, Pyridyl and pyrimidyl chalcogenolates of coinage metals and their utility as molecular precursors for the preparation of metal chalcogenides, *New J. Chem.*, 43, 11034–11040.

[13] Sharma, R.K., Wadawale, A., Kedarnath, G., Manna, D., Ghanty, T.K., Vishwanadh, B., and Jain, V.K., 2014, Synthesis, structures and DFT calculations of 2-(4,6-dimethyl pyrimidyl)selenolate complexes of Cu(I), Ag(I) and Au(I) and their conversion into metal selenide nanocrystals, *Dalton Trans.*, 43 (17), 6525–6535.

[14] Waitkins, G.R., and Clark, C.W., 1945, Selenium dioxide: Preparation, properties, and use as oxidizing agent, *Chem. Rev.*, 36 (3), 235–289.

[15] Reich, H.J., and Hondal, R.J., 2016, Why nature chose selenium, *ACS Chem. Biol.*, 11 (4), 821–841.

[16] Reddy, C.C., and Massaro, E.J., 1983, Biochemistry of selenium: A brief overview, *Fundam. Appl. Toxicol.*, 3 (5), 431–436.

[17] Zhang, M., Lu, J., and Weng, Z., 2018, Copper-catalyzed synthesis of 2,2-difluoro-1,3-benzoxathioles (selenles) and their insecticidial activities: The selenium effect, *Org. Biomol. Chem.*, 16 (24), 45558–4562.

[18] Santi, C., Jacob, R.G., Monti, B., Bagnoli, L., Sancineto, L., and Lenardão, E.J., 2016, Water and aqueous mixture as convenient alternative media for organoselenium chemistry, *Molecules*, 21 (11), 1482.

[19] Klayman, D.L., and Griffin, T.S., 1973, Reaction of selenium with sodium borohydride in protic solvent. A facile method for introduction of selenium into organic molecules, *J. Am. Chem. Soc.*, 95 (1), 197–199.

[20] Ibrahim, T.H., Chehade, Y., and Abou Zour, M., 2011, Corrosion inhibition of mild steel using Potato peel extract in 2 M HCl solution, *Int. J. Electrochem. Sci.*, 6, 6542–6556.

[21] Eid, A.M., Shaaban, S., and Shalabi, K., 2020, Tetrazole-based organoselenium bi-functionalized corrosion inhibitors during oil well acidizing: Experimental, computational studies, and SRB bioassay, *J. Mol. Liq.*, 298, 111980.

[22] Sehmi, A., Ouici, H.B., Guendouzi, A., Ferhat, M., Benali, O., and Boudjellal, F., 2020, Corrosion inhibition of mild steel by newly synthesized pyrazole carboxamide derivatives and HCl acid medium: Experimental and theoretical studies, *J. Electrochem. Soc.*, 167 (15), 155508.

[23] Ma Q., Qi, S., He, X., Tang, Y., and Lu, G., 2017, 1,2,3-Triazole derivatives as corrosion inhibitors for mild steel in acidic medium: Experimental and computational chemistry studies, *Corros. Sci.*, 129, 91–101.

[24] Parikh, K., and Joshi, D., 2013, Antibacterial and antifungal screening of newly synthesized benzimidazole-clubbed chalcone derivatives, *Med. Chem. Res.*, 22 (8), 3688–3697.

[25] Shubhalaxmi, S., Pathak, L., Ananda, K., and Bhat, K.S., 2016, Synthesis of focused library of novel aryloxyacids and pyrazoline derivatives: Molecular docking studies and antimicrobial investigation, *Cogent Chem.*, 2 (1), 1141388.

[26] Behbehani, H., and Ibrahim, H.M., 2012, 4-Thiazolidinones in heterocyclic synthesis: Synthesis of novel enaminones, azolopyrimidines and 2-arylimino-5-thiazolidinones, *Molecules*, 17 (6), 6362–6385.

[27] Katke, S.A., Amrutkar, S.V., Bhor, R.J., and Khairnar M.V., 2011, Synthesis of biologically active 2-chloro-*N*-alkyl/aryl acetamide derivatives, *Int. J. Pharma Sci. Res.*, 2 (7), 148–156.

[28] Hassan, A.H., 2016, Synthesis of chalcone derivatives and evaluation their biological activities, *J. Garmian Univ.*, 1 (10), 582–593.

[29] Saleh, T.A.K., 2017, Synthesis and characterization of chalcone derivatives from furfural, *Chem. Adv. Mater.*, 2 (4), 44–52.

[30] Hassan, A.F., Abdalwahed, A.T., Al-Luaibi, M.Y., and Aljadaan, S.A., 2021, Synthesis, characterization and thermal study of some new organochalcogenide compounds containing aryl group, *Egypt. J. Chem.*, 64 (9), 5009–5015.

[31] Maru, J., Patel, G.R., and Yadav, R., 2015, Spectral and microbial studies of some newly synthesized Schiff base derivatives of 2-(1*H*-benzo[d]oxazole-2-ylthio-*N*-(4-acetylphenyl)acetamide, *Int. Lett. Chem., Phys. Astron.*, 44, 57–65.

[32] Sladek, V., Rottmannová, L., Škorňa, P., Ilčin, M., and Lukeš, V., 2012, Theoretical 1H(Se-H) NMR shift in meta substituted Ph-XH (X = O, S, Se), *Acta Chim. Slovaca*, 5 (2), 159–163.

[33] Nikpour, S., Ramezanzadeh, M., Bahlakeh, G., Ramezanzadeh, B., and Mahdavian, M., 2019, *Eriobotrya japonica* Lindl leaves extract application for effective corrosion mitigation of mild steel in HCl solution: Experimental and computational studies, *Constr. Build. Mater.*, 220, 161–176.

[34] Daoud, D., Daouadi, T., Hamani, H., Chafaa, S., and Al-Noaimi, M., 2015, Corrosion inhibition of mild steel by two new S-heterocyclic compounds in 1 M HCl: Experimental and computational study, *Corros. Sci.*, 94, 21–37.

[35] Aslam, R., Mobin, M., Zehra, S., Obot, I.B., and Ebenso, E.E., 2017, *N,N*-Dialkylcystine Gemini and monomeric *N*-alkyl cysteine surfactant as corrosion inhibitors on mild steel corrosion in 1 M HCl solution: A comparative study, *ACS Omega*, 2 (9), 5691–5707.

[36] Manssouri, M., El-Ouadi, Y., Znini, M., Bouyanzer, A., Desjobert, J.M., and Majidi, L., 2015, Adsorption properties and inhibition of mild steel corrosion in HCl solution by the essential oil from fruit of Moroccan *Ammodaucus leucotrichus*, *Mater. Environ. Sci.*, 6 (3), 631–646.

[37] Salarvand, Z., Amirnasr, M., Talebian, M., Raeissi, K., and Meghdadi, S., 2017, Enhanced corrosion resistance of mild steel in 1 M HCl solution by trace amount of 2-phenyl-benzothiazole derivatives: Experimental, quantum chemical calculation and molecular dynamics (MD) simulation studies, *Corros. Sci.*, 114, 133–145.

[38] Adeyemi, O.O., and Olubomehin, O.O., 2010, Investigation of *Anthrocleista djalonensis* stem bark extract as corrosion inhibitor for aluminium, *Pac. J. Sci. Technol.*, 11 (2), 455–462.